Sequence-Specific Triple Helix Formation with Genomic DNA†

Zhaoyang Ye,‡ Ramareddy V. Guntaka,*,§ and Ram I. Mahato*,‡

Departments of Pharmaceutical and Molecular Sciences, University of Tennessee Health Science Center, Memphis, Tennessee 38163

Received March 26, 2007; Revised Manuscript Received June 17, 2007

ABSTRACT: We have previously demonstrated site-specific delivery of antiparallel phosphorothioate triplex forming oligonucleotide (TFO) specific to −165 to −141 promoter region of α1(I) collagen (abbreviated as APS165) to hepatic stellate cells (HSCs) of fibrotic rats after conjugation with mannose 6-phosphate-bovine serum albumin. However, we still need to determine whether there is correlation between transcription inhibition and triplex formation with genomic DNA. In this study, APS165 was modified with psoralen and the extent of triplex formation with α1(I) collagen DNA was determined in naked genomic DNA, isolated nuclei of HSC-T6 cells and whole cells by using a simple real-time PCR based method. In this method, a purification step was added to remove unbound APS165, which eliminated the possible artifacts during real-time PCR. Psoralen photoadduct formation was shown to be essential to retain triplex structure under denaturing conditions. On naked genomic DNA, 82.2% of DNA formed triplex and 36.7% of genomic DNA in isolated nuclei at 90 min contained triplex structure. As quantified by real-time PCR, 50% of genomic DNA in living cells at 12 h postincubation contained triplex structures. Furthermore, the triplex formation was dose-dependent with 26.5% and 50% of DNA having triplex structure at concentrations of 1 μM and 5 μM, respectively. Moreover, on a plasmid pCol-CAT220 containing rat α1(I) gene promoter (−225 to +113), 75.3% of triplex formation was observed, which was correlated with a 73.6% of transcription inhibition. These findings will further strengthen the therapeutic applications of APS165.

Oligonucleotides (ODNs[1]) can be designed to form triplex with double-stranded genomic DNA in a sequence-specific manner by binding in the major groove of the double strand via Hoogsteen hydrogen bonds between ODN bases and purine bases in the DNA targets that are already engaged in Watson−Crick hydrogen bonds (*1*−*3*). Triplex formation is known to occur at sequences containing a stretch of pyrimidines on one DNA strand and complementary purines on the other DNA strand. Depending on their base composition, triplex forming oligonucleotides (TFOs) bind in a parallel (for TFOs containing C and T nucleotides) or antiparrallel orientation (for TFOs containing G and A or T nucleotides) to the purine-containing strand of double stranded DNA. This provides a promising approach to the sequence-specific recognition of double-stranded DNA and subsequent gene regulation, including interfering with transcription, replication, repair and recombination (*2*, *4*−*7*). However, inhibition of gene expression (*8*−*10*) and induction of recombination (*11*) mainly relied on observations in mammalian cells using targets in exogenous DNA (plasmids). Recently, TFOs have also been shown to inhibit endogenous gene expression (*12*−*15*). Since DNA in cells is typically bound to histones and tightly packed into chromatin, the binding and activity of TFOs must be determined in this context. Chromatin structure is one of the major barriers since it may preclude TFO access to target sequences (*16*−*18*). Therefore, it is important to determine whether and how much of a triple helix complex can form at the target sequence to the genome *in vivo*. Many efforts to demonstrate triplex formation in chromosomal environment have been reported (*17*, *19*−*25*). However, conclusive evidence to show the triplex formation inside living cells is still needed to clarify the gene regulation mechanism of TFO molecules, since other mechanisms may be involved in TFO-induced gene inhibition and factors affecting triplex formation *in vivo* are still unclear. For example, views on the transcription dependence of triplex formation are inconsistent (*17*, *20*, *21*, *23*).

For detection of triplex formation in living cells, an additional barrier is the extremely low concentration of TFO in the nuclei of living cells, which resulted in many studies failing to show conclusively the triplex formation *in vivo* (*23*, *26*). To demonstrate triplex formation specificity and

† This work was supported by NIH Grants RO1 DK064633 (to R.V.G.) and RO1 EB003922 (to R.M.) and UT center grant, 47379 (to R.M.).

* Corresponding authors. R.I.H.: 26 S Dunlap Street, Feurt 413, Memphis, TN 38163; tel, (901) 448-6929; fax, (901) 448-6092; e-mail: rmahato@utmem.edu; http://cop.utmem.edu/rmahato. R.V.G.: 101 Molecular Science Bldg., Memphis, TN 38163; tel, (901) 448-8230; fax, (901) 448-8462; e-mail: rguntaka@utmem.edu.

‡ Department of Pharmaceutical Sciences.

§ Department of Molecular Sciences.

[1] Abbreviations: APS, antiparallel phosphorothioate; APS165, antiparallel phosphorothioate oligonucleotide specific to −165 to −141 promoter region of α1(I) collagen gene; BSA, bovine serum albumin; CAT, chloramphenicol acetyltransferase; DMEM, Dulbecco's modified Eagle's medium; DMN, dimethylnitrosamine; ECM, extracellular matrix; F, fluorescein; FBS, fetal bovine serum; GFP, green fluorescent protein; HSC, hepatic stellate cell; HSC-T6, immortalized rat hepatic stellate cell line; M6P-BSA, mannose 6-phosphate-bovine serum albumin; ODNs, oligonucleotides; PAGE, polyacrylamide gel electrophoresis; Pso, psoralen; SDS, sodium dodecyl sulfate; TE, Tris-EDTA; TFO, triplex forming oligonucleotide; UVA, ultraviolet irradiation at 366 nm.

10.1021/bi700580y CCC: $37.00
Published on Web 09/11/2007

efficiency either *in vitro* or *in vivo*, a variety of methods have been developed, including band shift assay (*9*), restriction enzyme protection assay (*27*, *28*), dimethyl sulfate (DMS) footprinting (*29*), competitive PCR (*20*), primer extension (*26*), single-strand ligation PCR (*21*), capture of triplex structures (*13*, *21*, *22*), and real-time PCR (*23*). Most of these studies were not done in living cells, and no consistent conclusions regarding triplex formation *in vivo* were drawn so far. Therefore, it is important to develop a simple, quantitative method to detect triplex formation inside living cells for reliable quantification. Psoralen is a bifunctional photoactive agent that has been used as a probe of nucleic acid structure and function and is minimally harmful to cellular constituents (*30*). Therefore, conjugation of photoreactive psoralen to a TFO at its 5′ end allows photoinduced cross-linking reaction of the psoralen at the specific sequence where the TFO binds to duplex DNA. To detect the triplex formation, psoralen conjugated TFO has been used extensively (*17*, *19*, *22*, *26*, *31*−*33*). Upon UV irradiation, psoralen introduces a covalent cross-link into the target DNA sequence which can effectively block transcription (*25*, *26*, *33*, *34*).

Fibrosis leads to organ dysfunction and is characterized by an excessive production of extracellular matrix (ECM) components, especially type I collagen (*35*). Therefore, inhibition of collagen synthesis should prevent fibrosis. We have demonstrated that different TFOs could form triplexes with the C1 region of the α1(I) collagen gene promoter (*9*, *36*) and inhibit transcription of α1(I) collagen gene promoter activity in fibroblasts in culture (*9*). We then successfully delivered these TFOs into hepatic stellate cells (HSCs) of fibrotic rats after conjugation with mannose 6-phosphate-bovine serum albumin (M6P-BSA) (*7*, *37*). In this study, we determined triplex formation of a psoralen modified TFO with target sequences (α1(I) collagen gene) in short duplex DNA, plasmid, naked genome, isolated nuclei, and intact cells by restriction enzyme protection, gel mobility shift assay, and PCR. We then quantified the extent of psoralen photoadducts using a simple real-time PCR based method. Finally, we determined inhibition of type α1(I) collagen gene transcription in an immortalized rat hepatic stellate cell line (HSC-T6 cells) (*38*). Our results indicate strong correlation between triplex formation and transcription inhibition of TFOs.

MATERIALS AND METHODS

Materials. Bovine serum albumin (BSA) (fraction V, purity >98%) was purchased from USB Corporation (Cleveland, OH). Spermidine and sucrose were purchased from Sigma-Aldrich (St. Louis, MO). Dulbecco's modified Eagle's medium (DMEM), penicillin G (5000 units/mL), streptomycin sulfate (5000 μg/mL), trypsin-EDTA, and Lipofectamine were purchased from Invitrogen Life Technologies (Carlsbad, CA). Heat-inactivated fetal bovine serum (FBS) was purchased from Atlanta Biologicals (Lawrenceville, GA). Restriction enzymes (*Xba*I, *Bgl*II, and *Bse*RI) were purchased from New England Biolabs (Ipswich, MA). MultiScirbe reverse transcriptase reagent and SYBR green-1 dye universal master mix were from Applied Biosystems Inc. (Foster, CA). Taq DNA polymerase and Wizard SV gel and PCR cleanup system were purchased from Promega (Madison, WI).

Oligonucleotides. The TFO (APS165) used in this study is a 25-nt antiparallel fully phosphorothioate ODN, specific to the promoter region (−165 to −141) of rat α1(I) collagen gene. APS165 and its control oligonucleotide MN (mismatched sequence) modified with 2-[4′-(hydroxymethyl)-4,5′,8-methylpsoralen]-hexyl-1-o-(2-cyanoethyl)-(*N*,*N*-diisopropyl)-phosphoramidite (Pso-APS165 and MN as indicated in Figure 1) were synthesized by Invitrogen Life Technologies (Carlsbad, CA), and the sequences of these ODNs are displayed in Figure 1. For cellular uptake experiments, APS165 was modified with 6-carboxyfluorescein (6-FAM: excitation, 495 nm; emission, 520 nm) at its 5′ end and was synthesized by Invitrogen Life Technologies (Carlsbad, CA), denoted as F-APS165. T1 and T2 are 30-nt ODNs used for forming duplex DNA fragment overlapping the triplex formation site in genomic DNA. T1 and T2 as well as primers (P1−P8 indicated in Figure 1) for PCR were obtained from Integrated DNA Technologies (Coralville, IA).

Plasmid Construction. A plasmid pCol-CAT220 containing the rat α1(I) gene promoter was constructed as described previously (*39*). Briefly, pCol 1.1 (constructed from pGEM-3Z vector (Promega, WI), containing rat α1(I) gene from −1000 to +113) was digested with *Xba*I and *Bgl*II to release a 338-bp fragment of the rat α1(I) gene (−225 to +113) and cloned into the *Xba*I−*Bam*HI site of the pCAT Basic vector (Promega, WI). pCol-CAT220 was transformed into Top10 competent cells. Colonies were grown in 50 μg/mL ampicillin containing LB agar plates, followed by growth of single colonies in ampicillin (50 μg/mL) containing terrific broth medium. After sufficient bacterial growth, the cells were pelleted by centrifugation followed extraction using Qiangen plasmid maxiprep kit as per vendor's protocol. Plasmid purity was assessed by UV spectrophotometry, agarose gel electrophoresis, and restriction digestion using *Xba*I and *Bgl*II enzymes.

UVA Treatment. UVA irradiation was done in a CAMAG UV cabinet with a UV lamp (100W) (CAMAG Scientific Inc, Wilmington, NC) set at 366 nm at a distance of 5 cm at 0 °C. The irradiation dose delivered to the samples was determined by a UV-meter, and the typical irradiance was ∼3.8 mW/cm^2 at a 5 cm source to target distance. UVA irradiation was used to generate photoadducts and thereby to covalently link the oligomers to their targets. After irradiation, triplex-dependent photoadducts were analyzed by restriction enzyme protection or PCR assays with or without purification.

Cell Culture. Immortalized rat liver stellate cells (HSC-T6) were kindly provided by Dr. Scott L. Friedman of Mount Sinai School of Medicine (New York, NY). Activated HSCs are the principal fibrogenic cell type in rat liver fibrosis (*38*). HSC-T6 cells were cultured in DMEM supplemented with 2 mM L-glutamine, 100 units/mL of penicillin, 100 mg/mL of streptomycin, and 10% of FBS at 37 °C and 5% (v/v) of CO_2.

Isolation of Genomic DNA. To isolate genomic DNA, HSC-T6 cells were harvested, resuspended in cell lysis buffer (20 mM Tris-HCl, pH 8.0, 150 mM NaCl, 2 mM EDTA and 1% sodium dodecyl sulfate (SDS)) containing 200 μg/mL proteinase K, and incubated at 55 °C for 4 h (*40*). Subsequently, the solution was extracted with an equal volume of phenol/chloroform mixture (v/v, 1/1) twice and chloroform once. After ethanol precipitation in the presence

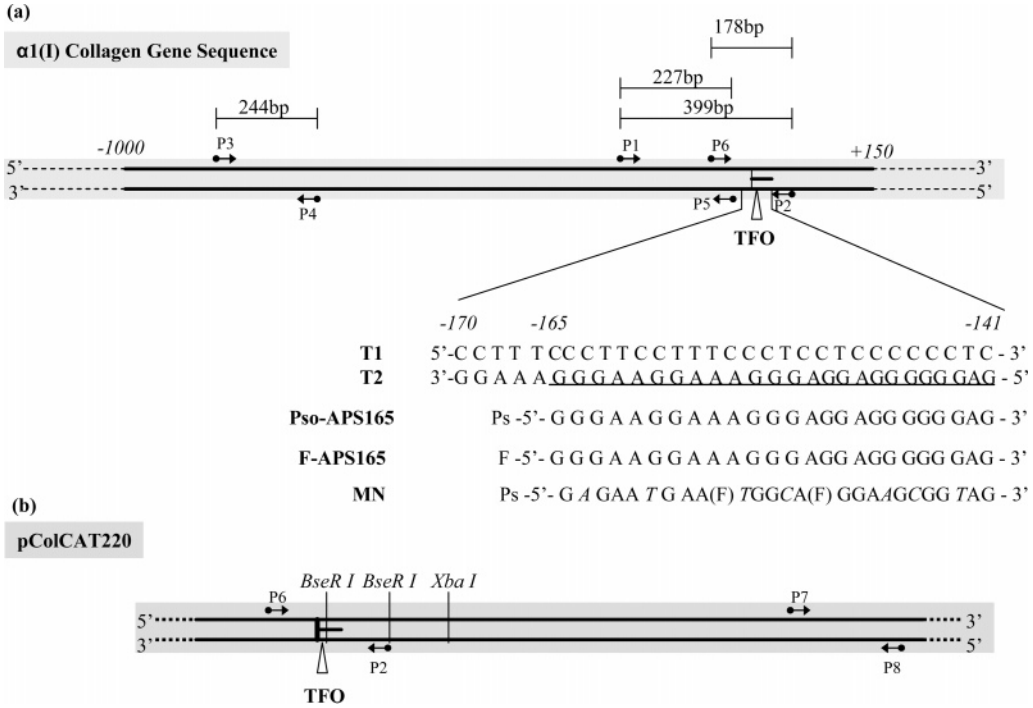

FIGURE 1: Target sequence and triplex forming oligonucleotides. (a) The promoter region of rat α1(I) collagen gene was shown. The triplex formation site of APS165 in the gene sequence (corresponding to positions between −165 and −141) was indicated. T1 and T2 are 30-nt oligonucleotides overlapping triplex formation site (underlined). Sequences of the triplex forming oligonucleotide APS165 and the control oligonucleotide MN (mismatched sequence, mismatched nucleotides highlighted in italics) are shown. Fluorescein (F) and psoralen (Pso) modifications in the sequences are indicated. APS165 is a 25-nt oligopurine and antiparallel to the target gene sequence. In addition, APS165 and MN are phosphorothioate modified oligonucleotides. P1−P6, positions of PCR-primers and the lengths of the PCR amplified fragments are indicated for the corresponding set of primers. (b) pCol-CAT220 containing a 338-bp fragment of the rat α1(I) collagen gene (−225 to +113) was shown with *Bgl*II, *Bse*RI, and *Xba*I restriction sites. Primers (P2 and P6−P8) were illustrated.

of 0.3 M of NaOAc (pH 5.5) at −80 °C for 30 min, the DNA pellet was collected by centrifugation at 16000*g* for 30 min at 4 °C. The pellet was resuspended in Tris-EDTA (TE) buffer (10 mM Tris-Cl, pH 7.5, 1 mM EDTA) containing 100 μg/mL RNase A and incubated at 37 °C for 1 h. The solution was again subjected to extraction with an equal volume of phenol/chloroform mixture (v/v, 1/1) twice and with chloroform once. The extracted DNA was precipitated with ethanol again and resuspended in DNase free water. The integrity of genomic DNA was checked on a 0.5% agarose gel, and its concentration was determined and the DNA was stored at −80 °C until use.

Restriction Enzyme Protection Assay. The specificity of triplex formation was studied *in vitro* using a restriction enzyme protection assay. pCol-CAT220 (2 μg; 0.63 pmol) was incubated with Pso-APS165 or MN (2 μg, Pso-APS165 or MN/plasmid: 300) in 10 μL of triplex forming buffer consisting of 20 mM Tris-HCl (pH 7.4), 20 mM $MgCl_2$, 2.5 mM spermidine, 10% sucrose, 0.25 mg/mL bovine serum albumin, and incubated at 37 °C for 90 min. The reaction mixtures were UVA-irradiated (5 J/cm^2) in order to covalently link TFOs bound to the target duplex via psoralen/UVA photoreactions. DNA was then purified by ethanol precipitation and subsequently digested with *Bgl*II, *Xba*I, and *Bse*RI restriction enzymes at 37 °C overnight. The extent of inhibition of *Bse*RI cleavage was assessed by 2% agarose gel electrophoresis.

Mobility Shift Assay. Triplex formation as well as photoadduct formation between psoralen modified APS165 and target duplex DNA *in vitro* was additionally analyzed in mobility shift assay. A 30-bp duplex DNA fragment was prepared by annealing equimolar amounts of complementary single-stranded oligonucleotides T1 and T2 (Figure 1). The mixture was heated at 80 °C for 5 min, incubated at 55 °C for 30 min, at 42 °C for 30 min, and then at room temperature for 30 min. To study the triplex formation using unmodified APS165, the duplex fragment (1.38 μg, 69 pmol) was incubated with increasing amounts of APS165 in 10 μL of triplex forming buffer at 37 °C for 90 min. Samples were analyzed using 15% native polyacrylamide gel electrophoresis (PAGE) in a buffer containing 89 mM Tris, 89 mM boric acid, pH 7.5, and 20 mM $MgCl_2$ at 8 V/cm at 4 °C for 5 h, and the gel was stained with ethidium bromide (*9*, *36*).

To study the photoadduct formation, the duplex fragment (50 ng, 2.5 pmol) was incubated with increasing amounts of Pso-APS165. The samples were then either not irradiated or irradiated with UV for 10 min at 0 °C. The samples were ethanol precipitated, resuspended in 20 μL of loading dye (95% formamide, 20 mM EDTA, 0.05% each bromphenol blue and xylene cyanol), and heated at 95 °C for 5 min. The resulting mixtures were assessed by denaturing polyacrylamide gel electrophoresis in 89 mM Tris (pH 8.3), 89 mM boric acid, 1 mM EDTA (15% polyacrylamide gel containing 7 M urea, 40% formamide), and methylene blue staining. Similarly, pColCAT220 (4 μg, 1.26 pmol) was incubated with 4 μg of Pso-APS165 or MN at the ODN/pDNA molar ratio of 300 in 10 μL of the triplex forming buffer, and then the mixtures were exposed to UVA treatment for different time intervals. The plasmid was then digested with *Bgl*II and *Xba*I to release a 338-bp fragment and separated on an 8% denaturing polyacrylamide gel.

Triplex Formation with Naked Genomic DNA. Two micrograms of genomic DNA isolated from HSC-T6 cells was incubated with various amounts (0.25 to 2.5 μM) of Pso-APS165 in 10 μL of triplex forming buffer for 90 min at 37 °C. The samples were then UVA irradiated for 10 min to allow photoadduct formation. The reaction mixtures were then subjected to PCR reaction using Taq DNA polymerase. The sequences of primers used in the experiments were P1, 5′-ATG AGA CAT GGC CAA GAG GAC CTT-3′; P2, 5′-TTT ATA CCA TCC TGA TGG AGG AGG GCT G-3′; and P5, 5′-TTT GCA ATT CTG CCA CCC TTG TCC-3′. P1 and P2 were used to amplify a 399-bp product overlapping the triplex formation region of the 25-bp α1(I) collagen fragment (Figure 1). On the other hand, P1 and P5 were used to amplify a 227-bp product in a nonrelated region, which was used as the internal control. The conditions for PCR reactions were as follows: 600 nM primers, 2.0 mM $MgCl_2$, 2.5 units of Taq polymerase, 2 min at 95 °C, followed by 35 cycles with 30 s at 94 °C, 50 s at 55 °C, 30 s at 72 °C. The PCR product was analyzed by 2% agarose gel electrophoresis.

Triplex Formation in Isolated Nuclei. The nuclei of HSC-T6 cells were isolated from cytoplasm as described previously (*37*) using NUCLEI PREP NUCLEI ISOLATION KIT (Sigma-Aldrich, St Louis, MO). The purity and number of isolated nuclei were determined under microscopy after dilution in trypan blue solution. Nuclei (5×10^6) were incubated with Pso-APS165 (10 μM) for 90 min at 37 °C in a 100 μL of triplex forming buffer with gentle rotation to avoid sedimentation of nuclei, and UVA-irradiated at 0 °C for 10 min. DNA was isolated from the nuclei as mentioned above. Two micrograms of DNA was subjected to PCR using primers P1 and P2 to amplify a 399-bp product overlapping the triplex formation of the 25-bp α1(I) collagen fragment (Figure 1). The PCR product was analyzed by 2% agarose gel electrophoresis.

Triplex Formation in HSC-T6 Cells. HSC-T6 cells were cultured in 6-well plates at 4×10^5 cells/well 24 h before treatment. Various amounts of Pso-APS165 (0, 1, and 10 μM) were incubated with cells in FBS-free DMEM at 37 °C for 12 h. For cross-linking formation, cells were washed, transferred to PBS, and irradiated with UV for 10 min at 0 °C. After irradiation, cells were harvested and genomic DNA was isolated as described above. Two micrograms of DNA was used for PCR reactions using primers P1 and P2. The PCR product was analyzed by 2% agarose gel electrophoresis.

Real-Time PCR. For quantitative assessment of the percentage of triplex formation on target DNA sequence, a real-time procedure was developed. All real-time PCR experiments were performed on ABI Prism 7700 Sequence Detection System using SYBR Green-1 dye universal master mix. After triplex forming reaction of Pso-APS165 or MN, with pCol-CAT220 (1 μg), genomic DNA (4 μg), nuclei or cells, DNA samples were prepared and subjected to purification by gel elution on 0.5% agarose gel for 10 min at 10 V/cm to separate unbound Pso-APS165 from plasmid or genomic DNA and extracted with Wizard SV gel and PCR cleanup system, because unbound TFO would interfere with the real-time PCR reaction. Aliquots of the purified DNA samples were subjected to real-time PCR with conditions: 600 nM primers, 2 min at 95 °C, followed by 40 cycles with 30 s at 94 °C, 50 s at 56 °C, 30 s at 72 °C. The primers for genomic DNA were P6, 5′-ACAAGGGTGGCAGAATTG-CAAAGG-3′, and P2, 5′-TTT ATA CCA TCC TGA TGG AGG AGG GCT G-3′, for overlapping triplex formation region as shown in Figure 2. At the same time, for the same sample, a control PCR reaction was also performed using another pair of primers outside the triplex formation region, P3, 5′-ACA GGC CTC CTG TAG CAA ATT CCA-3′, and P4, 5′-TGG CTC CAT GAA AGA CCC ACC TTT-3′. The primers for pCol-CAT220 were P6 and P2, and P7, 5′ -ATT CGC AAG ATG TGG CGT GTT ACG-3′, and P8, 5′-GGA AGC CAT CAC AAA CGG CAT GAT-3′. Similarly, P6 and P2 were used to amplify the sequence overlapping the triplex formation region and P7 and P8 were used in control PCR reactions. For a same DNA sample, the difference between the threshold cycle number from PCR reaction using primers for triplex formation region (Ct_T) and that from PCR reaction using primers for control region (Ct_C), $\Delta Ct = Ct_C - Ct_T$, was used to represent the amount of PCR product. The relative amount of PCR product was calculated by assuming the amount of PCR product of the control sample as 100%. The percentage of DNA containing triplex structure was thus calculated by subtracting the relative amount of PCR product from 100%.

Transfection of HSC-T6 Cells with TFOs. Before transfection experiments, HSC-T6 cells were cultured in 6-well plates at a density of 4×10^4 cells/well for 24h. TFOs were incubated with HSC-T6 cells in 1 mL of serum-free DMEM medium (final concentration of TFO to be 0.5 μM). TFO (F-APS165) was modified with 6-carboxyfluorecein (6-FAM) so that transfection as well as the intracellular localization of the fluorescence could be assessed by fluorescence microscopy. At 24 h post-transfection, cells were washed with ice-cold PBS buffer and mounted in Vectashield mounting medium containing 4,6-diamino-2-phenylindole (DAPI) (Vector Laboratories, Inc., Burlingame, CA), and the green fluorescence was visualized under a fluorescent microscope. Similarly, for isolated nuclei, F-APS165 was incubated for 90 min at 37 °C with mild vortex and fluorescence was observed as well.

Transcription Inhibition in HSC-T6 Cells. HSC-T6 cells were seeded in 6-well plates at 4×10^5 cells/well for 24 h until at 60−70% confluency before transfection experiments. To determine the effect of TFO on α1(I) collagen gene transcription, pCol-CAT220 was incubated with different amount of Pso-APS165 or APS165, UVA irradiated, and purified by gel elution on 0.5% agarose gel, and then 1.5 μg of DNA was transfected into HSC-T6 cells after complex formation with Lipofectamine at 3/1 (w/w) ratio. After 36 h incubation, total RNA was isolated using GenElute mammalian total RNA miniprep kit (Sigma, MO). cDNA was generated using MultiScirbe reverse transcriptase, and 100 ng of cDNA was amplified by real-time PCR using primers P7 and P8 (600 nM) under the condition as above to determine the transcription of the CAT gene. Simultaneously, 18S ribosomal RNA (18SrRNA) was also amplified using primers (forward, 5′-GTCTGTGATGCCCTTAGATG-3′; and reverse, 5′-AGCTTATGACCCGCACTTAC-3′) as internal control for real time PCR. Relative transcript levels were normalized to 18SrRNA. The data was presented by setting control sample with no Pso-APS165 treatment as 100%. To study the inhibition of gene expression by TFOs,

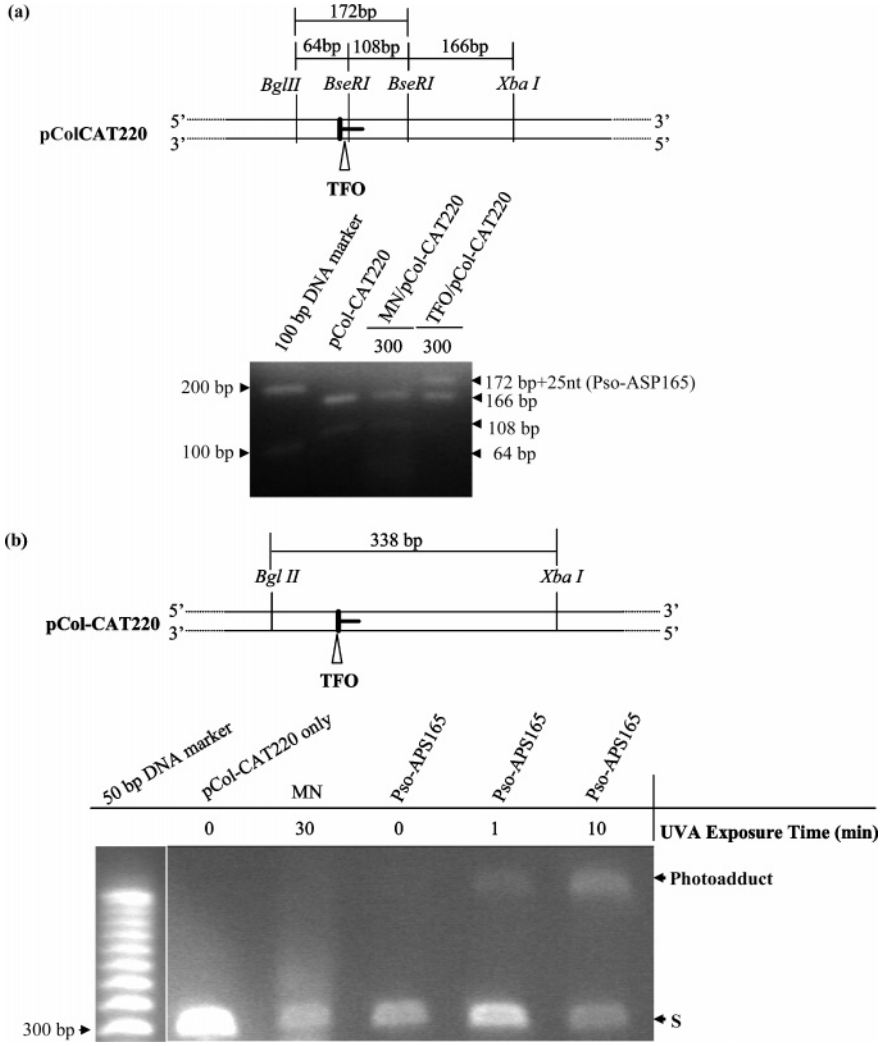

FIGURE 2: (a) Effect of TFO/pDNA ratio on triplex formation. pCol-CAT220 was incubated with Pso-APS165 at 300-fold molar excess. Following UV irradiation, the mixture was purified, and digested with *Bgl*II, *Bse*RI, and *Xba*I. The lengths of digested products (64bp, 166 bp, and 108 bp) are indicated. Inhibition of cleavage by *Bse*RI resulted in the disappearance of the 108-bp fragment and appearance of a new band of 172bp+25nt of APS165. (b) Time course of the reaction of Pso-APS165 with pCol-CAT220. pCol-CAT220 was incubated with Pso-TFO165 at 300-fold molar excess for 90 min at 37 °C, followed by UVA irradiation for 0, 1, and 10 min. The plasmid was then digested with *Xba*I and *Bgl*II to release a 338-bp fragment. The samples were finally applied to denaturing gel electrophoresis.

we also used pCol-GFP595 encoding green fluorescent protein (GFP) driven by human α1(I) collagen promoter from −495 to +100 (*36*). The TFO used here was an antiparallel phosphorothioate sequence (hC1APS, 5′-AGGGAAGG-GAGGAGGAGGGGGAGAGGTAAG-3′) reported before (*36*). However, the triplex was not preformed and we transfected HSC-T6 cells in two steps. First, HSC-T6 cells were transfected with pCol-GFP595 at a dose of 2 μg/well after complex formation with Lipofectamine at 3/1 w/w for 2 h. These cells were then transfected with hC1APS at different concentrations and incubated for a total of 36 h. GFP expression was determined by a fluorescence microscopy as well as by a fluorometer after protein extraction. Relative fluorescence intensity was normalized by total cellular protein, which was determined by bicinchoninic acid (BCA) protein assay kit (Pierce, IL).

RESULTS

Target and Psoralen-Linked TFOs. We have previously shown that the α1(I) collagen gene promoter contains two contiguous stretches of polypurine/polypyrimidine sequence between −141 to −200, which were the targets of the TFOs (*9*). While we reported triplex formation between the TFOs and short duplex DNA containing target sequences in α1(I) collagen gene promoter, we still need to demonstrate and quantify their triplex formation with genomic DNA.

As shown in Figure 1a, a 30-bp oligopyrimidine−oligopurine duplex sequence (T1:T2) from −141 to −170 in the C1 region of the α1(I) collagen gene promoter was chosen as a target sequence. We designed APS165 to study its triplex forming ability at this site. This oligonucleotide contains guanine and adenine nucleotides, allowing formation of G·G:C and A·A:T triplets, with (:) standing for Watson−Crick hydrogen bonds and (·) standing for reverse Hoogsteen hydrogen bonds after binding in an antiparallel orientation with respect to the purine strand of the duplex DNA. To increase the complexity of triplex formation microenvironment step by step, we demonstrated the triplex formation at the level of plasmid containing α1(I) collagen gene promoter, genomic DNA, isolated nuclei, and live cells.

We chose to use psoralen-conjugated TFOs because they can be photoinduced to become irreversibly bound to their

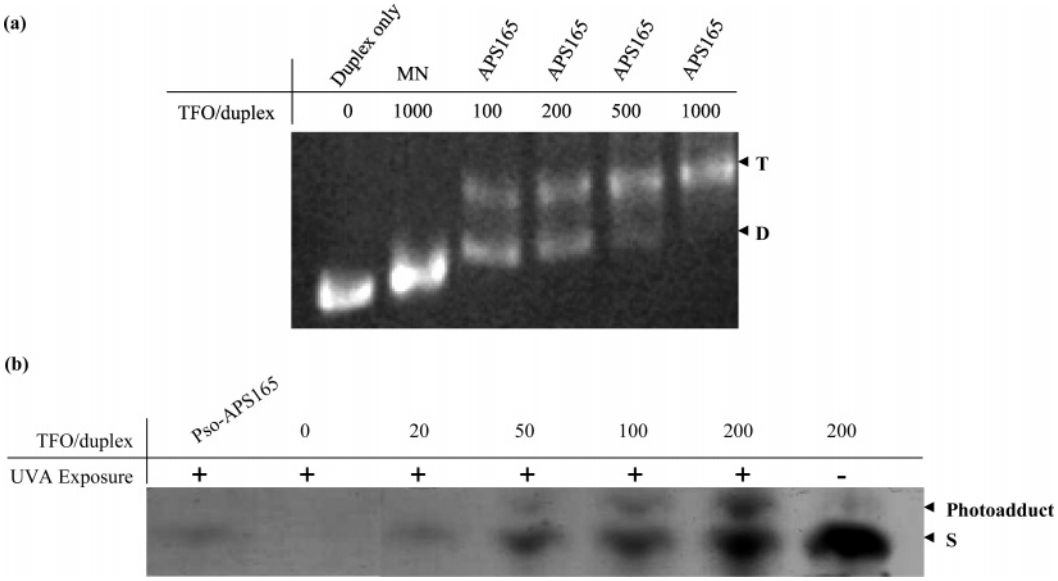

FIGURE 3: Triplex formation between APS165 with C1 duplex DNA. (a) Effect of TFO/duplex DNA ratio on triplex formation. The formation of duplex and triplex was checked by electrophoresis on a native polyacrylamide gel. (b) Effect of TFO/duplex ratio and UVA exposure on psoralen-induced photoadduct formation between Pso-APS165 and duplex DNA. Irradiation was carried out for 10 min at 0 °C at 366 nm. Photoadduct was checked by electrophoresis on a 15% denaturing polyacrylamide gel containing 7 M urea and 40% formamide.

target DNA sequence so that triplex structure can be retained intact until detection during sample preparation (*13*). Even though the triplex structure is pretty stable after formation (*9*), the triplex structure might be destroyed during the very harsh sample preparation steps (i.e., purification), which will lead to underestimation of the triplex formation ability. TFOs were conjugated to psoralen C_6 phosphoramidite via a six-carbon linker to allow UV-induced photoadduction after triplex formation at the target site. To demonstrate sequence-specific binding activity of the TFO, one control oligonucleotide MN with 7 nucleotides mismatched was also designed and included in experiments (Figure 1a).

In Vitro Characterization of Triplex Formation. Specificity of triplex formation between target DNA and APS165 was examined with a restriction enzyme protection assay that is based on the ability of triplex structures to interfere with restriction enzyme cleavage. pCol-CAT220 was used to form triplex with APS165. The triplex target sequence overlapped with a *Bse*RI cleavage site (Figure 2a). Three-hundred-fold molar excess of Pso-APS165 was incubated with pCol-CAT220. After digestion with *Bgl*II, *Bse*RI, and *Xba*I restriction enzymes, three fragments of 166 bp, 108 bp, and 64 bp should be generated without protection (Figure 2a). So, without incubation with Pso-APS165 or at the presence of control oligonucleotide MN (Figure 2a), we observed 166-bp and 108-bp fragments and due to much lower intensity, 64-bp fragment was not showing up. In contrast, inhibition of *Bse*RI by triplex structure resulted in the disappearance of the 108-bp fragment at the Pso-APS165/pCol-CAT220 of 300 and a new fragment appeared which was corresponding to fragment of 108 bp plus 64 bp and bound 25-nt Pso-APS165. This suggests that the *Bse*RI site was protected by Pso-APS165 and the observed inhibition was sequence-specific.

To determine the effect of UVA irradiation time on photoadduct formation, pCol-CAT220 was incubated with Pso-APS165 or MN at 300-fold-molar excess for 90 min at 37 °C followed by UVA irradiation for 0, 1, and 10 min in the case of Pso-APS165 and 30 min in the case of MN. Following UVA irradiation, Pso-APS165 bound pCol-CAT220 was digested with *Xba*I and *Bgl*II to release a 338-bp fragment containing triple helix. On the denaturing gel, the photoadduct could not dissociate and the TFO was attached to the target sequence leading to appearance of a new slower-migrating species (corresponding to DNA containing triplex structure). As can be seen in Figure 2b, the band intensity of the new species increased with increase in the UVA irradiation time, with almost half of the original DNA transformed into new species. In contrast, the control oligonucleotide MN did not show any triplex formation even at 30 min post UVA irradiation (Figure 2b).

Triplex Formation with α1(I) Collagen DNA Duplex. To determine the triplex formation ability of APS165 with a target duplex sequence (T1:T2), triplex formation was characterized in mobility shift assays. The 30-bp α1(I) collagen DNA fragment from −141 to −170 (T1:T2) (1.38 μg/sample) was incubated with APS165 or control oligonucleotide MN at increasing TFO/duplex DNA molar ratios, followed by gel electrophoresis on 15% native polyacrylamide gel (Figure 3a). Unlike the control oligonucleotide MN, which did not form triplex with the α1(I) duplex, the APS165 formed triplex with the target duplex, and the amount of triplex DNA structure increased with increase in their molar ratios based on the band intensity with ethidium bromide staining. At the molar ratio of 200 (TFO/duplex DNA), almost half of the duplex was transformed into triplex structure and all the duplex was transformed into triplex at the ratio of 1000 for APS165 (Figure 3a).

We then determined the effect of molar ratios of Pso-APS165/duplex on psoralen−DNA photoadduct formation upon UVA irradiation. In this case, the 30-bp duplex DNA (50 ng, 2.5 pmol) was incubated with increasing amounts of Pso-APS165, UVA-irradiated for 10 min and applied to 15% denaturing polyacrylamide gel electrophoresis. Fast-migrating species was single-stranded Pso-APS165, and no

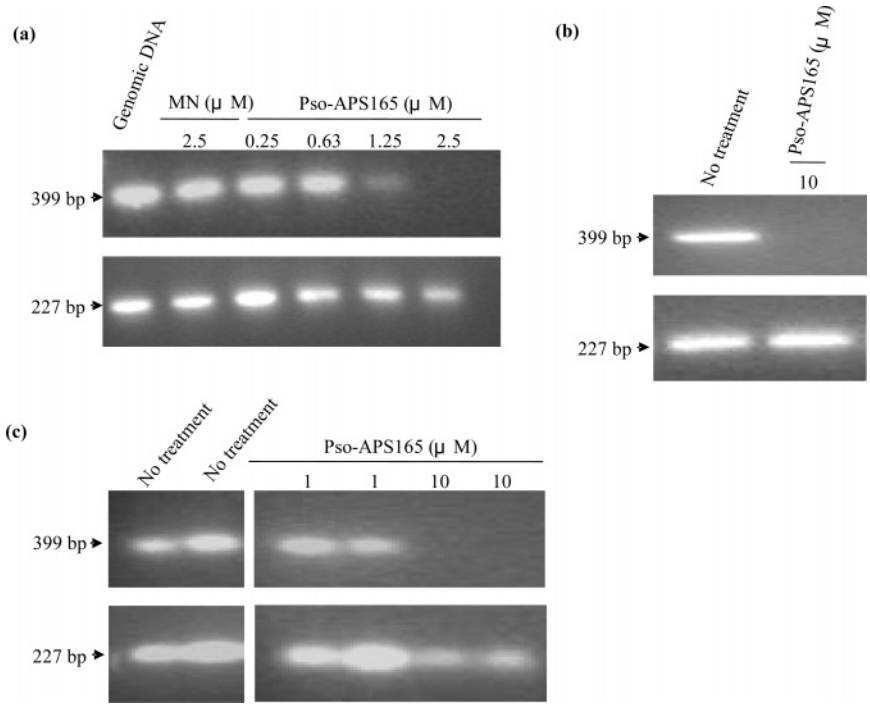

FIGURE 4: Triplex formation with genomic DNA, isolated nuclei, and living cells. (a) Genomic DNA was incubated with Pso-APS165 or control oligonucleotide MN. Samples were then UVA irradiated for 10 min and then subjected to PCR reaction without any manipulation. (b) Isolated nuclei were incubated with or without 10 μM Pso-APS165 for 90 min at 37 °C with gentle rotation, and UVA irradiated at 0 °C. The nuclei were then digested and DNA was isolated. The isolated DNA (2 μg) was subjected to PCR amplification using primers P1 and P2. (c) HSC-T6 cells were incubated with or without Pso-APS165 at 37 °C for 12 h and UVA irradiated, and the cells were harvested to isolate genomic DNA, which was subjected to PCR reactions. The PCR products were analyzed by 2% agarose gel electrophoresis.

staining appeared for 50 ng of duplex DNA (Figure 3b). We noticed that, with increasing Pso-APS165/duplex DNA ratios, the fraction of slower migrating species increased for samples with UV-irradiation, and a significant large fraction of Pso-APS165 was converted into a slower-migrating species at the Pso-APS165/duplex DNA ratio of 200 (Figure 3b). However, no slower-migrating species was seen even at the TFO/duplex ratio of 200 in the absence of UVA-irradiation. In contrast to Figure 3A, since we used denaturing gel which could destroy the hydrogen bonds among DNA bases, the triplex structure could not be retained without psoralen-dependent photoadduct. Since photoadduction of psoralen-conjugated TFO with the target DNA is irreversible under the condition of denaturing gel electrophoresis, it would prevent dissociation of TFO from the DNA duplex. However, we did not differentiate the monoadduct and cross-linking, since in our quantification method, both forms of photoadducts will inhibit PCR reaction.

Triplex Formation with Genomic Target DNA. As a next step, we determined the ability of TFOs to specifically bind to α1(I) collagen promoter in the natural context of purified genomic DNA. Different amounts of Pso-APS165 were incubated with 2 μg of purified genomic DNA isolated from HSC-T6 cells for 90 min at 37 °C and UVA irradiated for 10 min to allow photoadduct formation. Primers P1 and P2 were used to amplify the 399-bp product overlapping the triplex formation region of the 25-bp α1(I) collagen, while P1 and P5 were used to amplify a 227-bp fragment in a nonrelated control region. If the triplex is formed on genomic DNA, the TFO can be covalently attached to the double helix via psoralen−DNA photoadduct formation. Psoralen−DNA photoadducts obtained after treatment with Pso-APS165 and UVA irradiation are not substrates for PCR amplification using primers located on each side of the psoralen photoadduct site (*23*, *26*) implying that a triplex structure in the genomic DNA did not allow PCR amplification of 399-bp fragment overlapping α1(I) collagen target sequence. We could see the significant reduction of PCR product when 1.25 and 2.5 μM of Pso-APS165 were used (Figure 4a). In contrast, for the same sample, amplification of a 227-bp product in an unrelated distal region by PCR was minimal. In addition, when 2.5 μM MN was incubated with the same amount of genomic DNA, PCR reaction was not affected. These results demonstrate the ability and specificity of triplex formation of Pso-APS165 with purified genomic DNA *in vitro*.

Triplex Formation in Isolated Nuclei. The ability of Pso-APS165 to bind to the genomic target in its intact supranucleosomal structure was tested by incubating 10 μM Pso-APS165 with 5×10^6 of isolated nuclei of HSC-T6 cells in 100 μL of triplex forming buffer for 90 min at 37 °C and then UVA irradiated for 10 min. No PCR product was detected when the genomic DNA isolated from the UVA-irradiated nuclei was subjected to PCR reaction using primers P1 and P2 to amplify a 399-bp product containing α1(I) collagen target site (Figure 4b). However, without Pso-APS165 a high amount of PCR product was observed. The results suggested that Pso-APS165 formed a substantial amount of triplex-dependent photoadducts in nuclei and inhibited PCR amplification in this specific region. This indicated the accessibility of the α1(I) collagen target sequence in the intact supranucleosomal structure to Pso-APS165.

Triplex Formation in HSC-T6 Cells. It is well-known that ODNs possess low ability to penetrate the cellular/intracellular membranes to get entry into cytoplasm, but are known

to passively diffuse through the nuclear pore into the nucleus once they are escaped from the endosome/lysosome vesicles. Therefore, HSC-T6 cells were incubated with 0, 1, and 10 μM of Pso-APS165 for 12 h at 37 °C. The cells were then UVA-irradiated for 10 min, and genomic DNA was isolated and subjected to PCR using primers P1 and P2 to amplify the 399-bp fragment containing triplex formation site. No significant PCR product was seen when the cells were incubated with 10 μM Pso-APS165 (Figure 4c). In contrast, nontreated cells as well as the cells incubated with 1 μM Pso-APS165 showed a similar band intensity representing the 399-bp PCR product.

Quantification of Triplex Formation by Real-Time PCR. To characterize triplex formation in a quantitative manner in different chromatin contexts, we developed a real-time PCR-based approach that allows quantification of triplex formation with the target site in the genome. This approach allowed us to determine the DNA amount in unknown samples. Since triplex structure would inhibit PCR reaction, we could measure the amount of those DNA molecules without triplex structure. In other words, we could determine the amount of DNA containing triplex structure using real-time PCR. To avoid the possible interference of unbound TFO with the real-time PCR process, we purified plasmid or genomic DNA from the triplex forming reaction mixture and then aliquots of the samples were applied for PCR.

Compared to genomic DNA, pCol-CAT220 contained a much larger amount of target sequence of Pso-APS165, which would be easier for detection. One microgram of pCol-CAT220 was incubated with different amount of Pso-APS165 and then UVA-irradiated. After purification, one twentieth of the sample DNA (~10 ng) was used for PCR reaction. By calculating ΔCt from the two PCR reactions using two sets of primers (P6/P2 and P7/P8) for the same sample as we mentioned in Materials and Methods, the amount of PCR product relative to the control sample (in which pCol-CAT220 was not incubated with Pso-APS165) could be determined (Figure 5a). We observed a dose-dependent reduction in the amounts of PCR product when pCol-CAT220 was incubated with different amounts of Pso-APS165. More specifically, with 1 μg (12.5 μM) and 2 μg (25 μM) of Pso-APS165 (Pso-APS165/plasmid molar ratio: 300 and 600), PCR products were 76.3% and 24.7%, which meant 23.7% (= 100% − 76.3%) and 75.3% (= 100% − 24.7%) of the plasmid containing triplex structure, respectively. However, when UVA-irradiation was omitted, only 48.9% (= 100% − 51.1%) of the plasmid was detected to contain triplex structure with 25 μM Pso-APS165, indicating the loss of triplex structures during sample preparation without psoralen photoadduct formation.

Similarly, genomic DNA was also incubated with Pso-APS165 and purified by gel elution. However, 4 μg of genomic DNA was used since the content of target sequence would be much lower compared to pCol-CAT220 and the gel extraction efficiency was also lower (~10%) compared to that of plasmid DNA (data not shown). As shown in Figure 5b, the relative amount of PCR product was 34.6% and 17.8% with 25 μM (2 μg) and 50 μM (4 μg) of Pso-APS165, respectively. In other words, the amount of the genomic DNA containing triplex structure was 65.4% (= 100% − 34.6%) and 82.2% (= 100% − 17.8%), respectively. This confirmed the dose-dependent triplex formation as we observed with

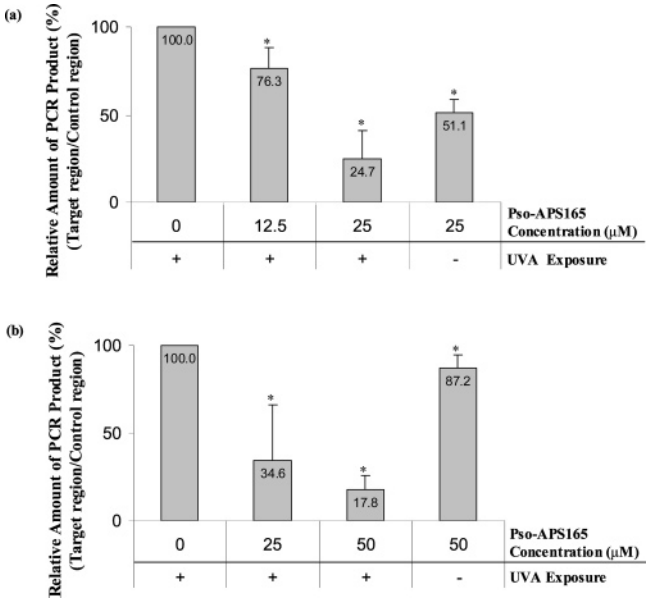

FIGURE 5: Quantitative measurement of triplex formation *in vitro*. (a) pCol-CAT220 (1 μg) was incubated with different amounts of Pso-APS165. Samples were then UVA irradiated for 10 min, and then the mixture was subjected to 0.5% agarose gel elution and extraction. Aliquots were subjected to real-time PCR. (b) Genomic DNA (4 μg) was incubated with different amounts of Pso-APS165. Samples were then UVA irradiated for 10 min, and then the mixture was subjected to 0.5% agarose gel elution and extraction. Aliquots were subjected to real-time PCR. The amounts of PCR products of target fragments were calculated based on difference between Ct numbers obtained for the same sample from a control region and target region. Relative PCR product was reported as a function of Pso-APS165 concentration by setting sample without TFO treatment as 100%. Data were expressed as the mean ± standard deviation (SD) ($n = 3$). *: $P < 0.05$ was considered statistically significant. Statistics were calculated based on unpaired Student's *t* test (+, with UVA irradiation; −, without UVA irradiation).

pCol-CAT220. Similarly, when UVA-irradiation was omitted, we detected only 12.8% of the DNA containing triplex structure even at 50 μM Pso-APS165. This indicates that during sample preparation the bound TFO was most likely lost without psoralen photoadduct formation, which again confirmed the necessity of using psoralen modification in the quantification experiments.

When we applied the quantification method to DNA samples from nuclei which were treated with Pso-APS165 under different conditions as indicated in Figure 6a, it was found that, by incubating for 90 min at 5 μM and 10 μM in 100 μL of triplex forming buffer with Pso-APS165, 15.1% and 36.7% of genomic DNA in isolated nuclei contained triplex structure, respectively. Again, without UVA-irradiation, it was only 22.6%. Quantification in living cells was very successful. After incubation of 12 h with Pso-APS165, 26.5% and 50% of DNA from HSC-T6 cells were found to have triplex structure at concentrations of 1 μM and 5 μM, respectively (Figure 6b). However, for APS165 without psoralen modification, the triplex structure detected was much lower (20.3% compared to 50% at 5 μM). When we compared the triplex formation between in nuclei and in living cells, the extent of triplex formation is somewhat lower in isolated nuclei (36.7% compared to 50% in living cells), probably due to the shorter incubation time (90 min) compared to that for living cells (12 h).

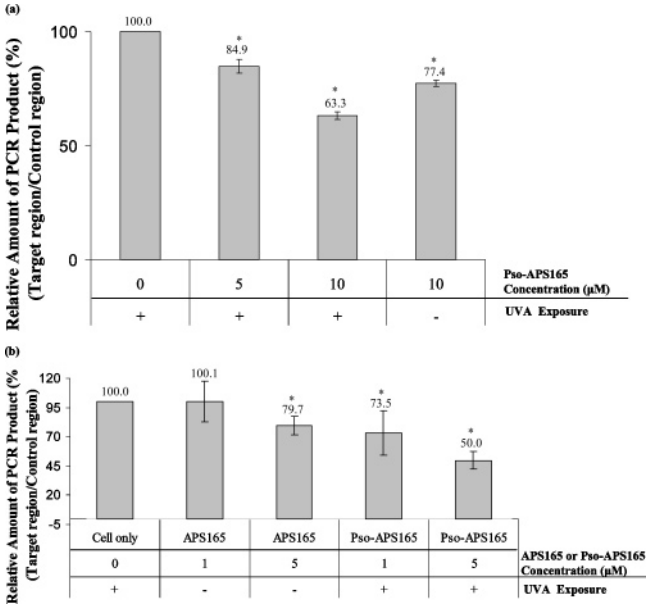

FIGURE 6: Quantitative measurement of triplex formation in nuclei and living cells. (a) Isolated nuclei were incubated with Pso-APS165 at concentrations of 0, 5, and 10 μM for 90 min at 37 °C. The nuclei were then UVA irradiated for 10 min, and then genomic DNA was isolated and purified. Aliquots of DNA samples were subjected to real-time PCR. (b) HSC-T6 cells were incubated with Pso-APS165 or APS165 at concentrations of 0, 1, and 5 μM at 37 °C for 12 h and UVA irradiated, and the cells were harvested to isolate genomic DNA. The DNA was purified by gel elution, and aliquots were subjected to real-time PCR. The amounts of PCR products of target fragments were calculated based on difference between Ct numbers obtained for the same sample from a control region and target region. Relative PCR product was reported as a function of Pso-APS165 concentration by setting sample without TFO treatment as 100%. Data were expressed as the mean ± standard deviation (SD) ($n = 3$). *: $P < 0.05$ was considered statistically significant. Statistics were calculated based on unpaired Student's t test (+, with UVA irradiation; −, without UVA irradiation).

Cellular Uptake and Nuclear Translocation of TFO. The ability of APS165 to be taken up by cells was studied. APS165 was labeled with 6-FAM (F-APS165). In Figure 7, under fluorescence microscopy, a significant intensity of green fluorescence was found to be associated with nuclei (blue) at 24 h post-transfection of F-APS165. When F-APS165 was directly incubated with isolated nuclei, a high intensity of green fluorescence could be quickly found to be inside the nuclei. In an expanded view, the association of F-APS165 with nuclear structure was more obvious. These results confirmed that APS165 could gain access into nuclei in living cells by direct incubation without any transfection reagent.

Inhibition of α1(I) Collagen Transcription in HSC-T6 Cells. As shown in Figure 8a, the gene transcription of pCol-CAT220 was highly inhibited by preformed triplex. We observed dose-dependent inhibition with increased Pso-APS165/plasmid molar ratios. Compared to control sample without Pso-APS165 treatment, the relative CAT mRNA levels were 43.8%, 31.9%, and 26.4% when triplex was preformed at 100, 300, and 600 of Pso-APS165/plasmid molar ratio, which were corresponding to 56.2%, 68.1%, and 73.6% of inhibition, respectively. Similarly, in another experiment, when we first transfected HSC-T6 cell with pCol-GFP595 complexed with Lipofectamine and then with a TFO hC1APS, we also observed a decrease in GFP gene expression in a dose-dependent manner (Figure 8b). Using fluorescence microscopy, the GFP expression was easily monitored (panels 1−4). The intensity of fluorescence was measured using a fluorometer after cell lysis. The highest inhibition of GFP gene expression was found to be 87.8% when HSC-T6 cells were treated with 1 μM TFO. However, this high gene inhibition at only 1 μM is probably due to the residual of Lipofectamine in the culture media, which has been formulated with pCol-GFP595.

DISCUSSION

In the promoter region of α1(I) collagen gene, the entire region spanning from −140 to −200 exists as an asymmetric polypurine−polypyrimidine tract in which the polypyrimidine sequence at −141 to −170 is called C1 regions, which is localized on the noncoding strand, whereas the adjacent polypurine sequence from −171 to −200 is called C2 region, which is present on the coding strand (*39*). The *cis*-acting elements in the C1 and C2 regions plays a key role in collagen transcription, and hence makes it an ideal target for developing antigene-based antifibrotic agents (*41*, *42*). We have demonstrated that TFOs could form triplex in this region and inhibit activity of the promoter *in vitro* (*9*, *36*, *39*). In addition, TFOs have been shown to prevent/reverse fibrosis in a dimethylnitrosamine (DMN) induced liver fibrosis model in rats, which indicated the therapeutic potential of these TFOs (*7*). However, thorough understanding of *in vivo* triplex formation ability and efficiency of these TFOs is still essential for their use as antifibrotic agents.

Most of studies on specificity, efficiency, stability, and bioactivity of TFO-induced triplex formation are based on *in vitro* targets in short duplex DNA, constructed plasmids (*8*−*10*, *26*, *28*, *31*, *33*). However, based on these *in vitro* results, it is not possible to correlate triplex formation with transcription inhibition of TFOs *in vivo*. Therefore, determination of chromosomal binding of TFOs is desirable in the development of an antigene strategy. Using pCol-CAT220, we could explicitly correlate the extent of triplex formation with the degree of transcription inhibition. At the same triplex formation condition (TFO/plasmid = 600), 73.6% of gene inhibition was seen at 75.3% of triplex formation. Furthermore, with genomic DNA in living cells, we showed 26.5% and 50% of triplex formation at 1 and 5 μM of Pso-APS165, respectively. This was also consistent with our previous results (*37*), where we showed that at 0.5 μM of free TFO did not inhibit type α1(I) collagen gene transcription and with transfection reagent (i.e., Lipofectamine or conjugated with M6P-BSA), around 50% of gene inhibition was observed at 0.5 μM and 80% at 1 μM. This was because conjugation of TFO with M6P-BSA increased its cellular uptake by almost 10-fold at 6 h postincubation (*37*). In isolated nuclei, 36.7% of triplex formation was observed, possibly due to less incubation time (90 min). However, these results suggest that there is no intrinsic cellular limitation to TFO binding besides the chromatin structure at the target site (*23*). By simply increasing delivery of TFOs, the triplex formation as well as bioactivity could be significantly improved (*7*, *37*, *43*). Even though TFO was poorly taken up by HSC-T6 cells, we could still observe a significant amount of TFO associated with nuclear structure after 12−24 h incubation with intact

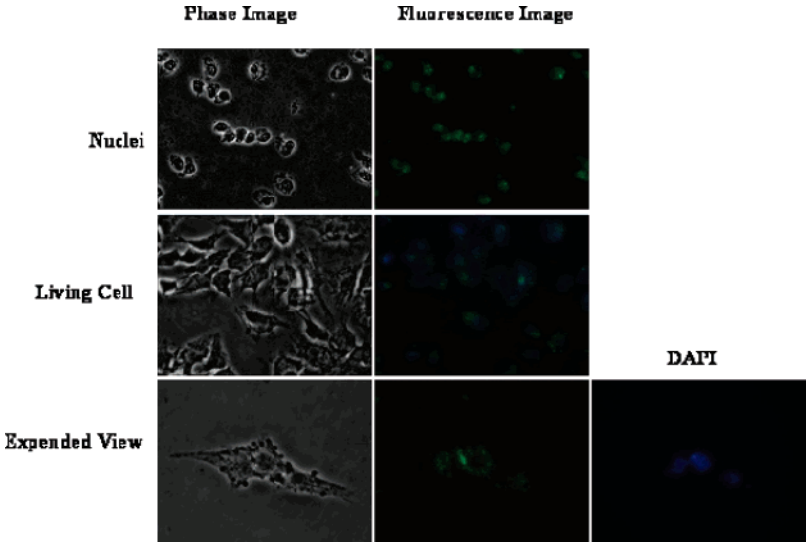

FIGURE 7: Cellular and nuclear uptake of APS165. Isolated nuclei of HSC-T6 cells and living HSC-T6 cells were incubated with F-APS165 for 90 min and 24 h, respectively. HSC-T6 cell nuclei were stained with DAPI and visualized under fluorescent microscopy (DAPI, blue; 6-FAM, green).

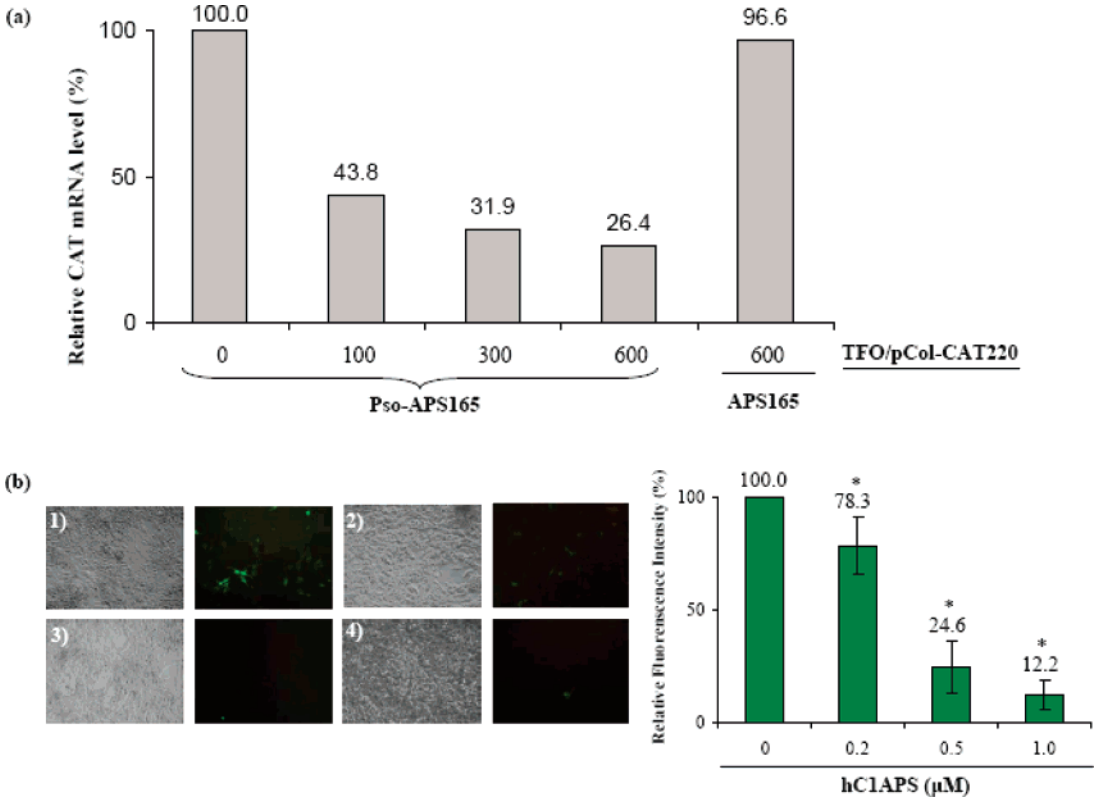

FIGURE 8: Transcription inhibition. (a) Relative transcription of CAT gene of pCol-CAT220 under the control of rat α1(I) collagen gene promoter. pCol-CAT220 was incubated with Pso-APS165 or APS165 at different ratios as indicated, UVA irradiated, purified by gel elution, and transfected into HSC-T6 cells after complex formation with Lipofectamine at 3/1 (w/w) ratio. After 36 h incubation, total RNA was isolated. cDNA was generated and amplified by real-time PCR. Ct value was normalized by that of 18s RNA. The data was presented by setting control sample with no Pso-APS165 treatment as 100%. (b) Relative expression of GFP in HSC-T6 cells transfected with Lipofectamine/pCol-GFP595 complexes, followed by incubation with hC1APS. GFP expression was determined by visualizing transfected cells under a fluorescent microscopy (panels 1−4) and relative fluorescent intensity of cell extract by a fluorometer. hC1APS concentrations: 0, 0.2, 0.5, and 1.0 μM for panels 1 to 4, respectively. GFP expression levels were normalized by measuring total protein concentration by BCA assay. Data were expressed as the mean ± standard deviation (SD) ($n = 3$). *: $P < 0.05$ was considered statistically significant. Statistics were calculated based on unpaired Student's t test.

HSC-T6 cells and when TFO was incubated with nuclei, we found that it quickly accumulated in nuclei (Figure 7). However, triplex formation in nuclei as well as living cells was possible only when pretty high concentrations of TFOs were used. We could detect the triplex formation by incubating HSC-T6 cells with 10 μM of Pso-APS165 without any transfection reagent but not at 1 mM using conventional PCR (Figure 4c). In our settings, quantification of triplex

formation in living cells showed 50% of genomic DNA containing triplex structure at optimized conditions, which indicated that intracellular conditions were favorable for the existence of triplex (*29*, *33*). However, another intriguing issue is whether noncovalently bound triplex itself can inhibit gene expression. Based on results from many other studies (*13*, *33*) and this study (Figure 8b), it is clearly suggested that in *in vivo* situation, APS165 could persist in cells or blockade the activity of RNA polymerase.

Our result of 50% triplex formation *in vivo* is comparable to two other studies (*20*, *23*). However, many other reported 1−50% triplex formation in living cells (*17*, *21*−*23*). This suggests that triplex formation is dependent on cell types, binding affinity and metabolic stability of TFOs, accessibility of chromosomal DNA targets, and detection methods. It has been shown that triplex formation could be affected by transcription activity (*17*, *23*), and cell cycle (*24*). In addition, repair of psoralen photoadducts inside the cells could also happen (*33*). Different detection methods may also contribute to the wide variation in the degree of triplex formation *in vivo*. In our PCR strategy, we amplified a control region and a target region and these two regions are only separated by several hundred base pairs. The psoralen cross-linking possibly prevents the dissociation of double strands of DNA in the control region completely, which might compete with primer annealing (*26*), and thus it might result in underestimation of the triplex formation in our settings leading to possible artifacts. However, since in our target sequence there is no 5′-TpA-3′ sequence adjacent to the 5′-end of Pso-APS165, a preferential site for psoralen-induced cross-linking (*32*), and irradiation was done at 366 nm, the fraction of mono-photoadducts must be very high. The competition of primer annealing in the control region might not be significant. Therefore, we did observe marginal inhibition of amplification in the control region but not significant (Figure 4a).

Capture and detection of triplex structures from a reaction mixture remain another challenge, which requires a highly sensitive quantification method. Giovannangeli et al. (*20*) could detect the triplex formation in permealized cells by using the combination of DNase I protection and Southern blot assays and competitive PCR. However, this is pretty tedious and not sensitive enough for quantification. Besch et al. (*22*) also developed a PCR based method, in which the triplex structure was first enriched by using streptavidin-coated magnetic beads and then DNA sample was subjected to a two step PCR reaction (a conventional PCR followed by a real-time PCR) for quantification. These authors quantified the triplex structures in living cells which was less than 1%, suggesting the need to develop new strategies to improve the triplex formation in living cells. These strategies include TFO analogues with high binding affinity (*19*, *44*, *45*) and efficient delivery strategies (*7*, *37*, *43*). In addition, psoralen modified TFO has been used for assessing triplex formation (*17*, *22*, *26*, *31*, *32*). In contrast, Debin et al. have failed to demonstrate triplex formation in intact cells when using non-psoralen modified TFO (*29*). We began with a 30-bp duplex target of −170 to −141 promoter region of α1(I) collagen gene, since this is the simplest target for APS165. As shown in Figure 3a, APS165 could efficiently form triplex with half of the duplex transformed to triplex at the molar ratio of 200 (TFO/duplex). This finding is in good agreement with our previously published results for different TFOs targeted to the C1 region of α1(I) collagen gene, in which radiolabeled duplex DNA was used (*9*). The specificity of triplex formation was confirmed by including a control oligonucleotide MN, which was different from APS165 with 7 nucleotides. However, only the psoralen photoadduct when using Pso-APS165 could survive under the conditions of denaturing PAGE (Figure 3b). This suggests that psoralen-induced photoadduct could protect the triplex structure against harsh conditions during sample preparation in which the formed triplex otherwise might be destroyed. The enzyme protection assay further confirmed the efficiency and specificity of triplex formation of Pso-APS165 (Figure 2a). The specificity of APS165 was further confirmed from results using conventional PCR to demonstrate the triplex formation of naked genomic DNA with Pso-APS165 but not with MN (Figure 4a).

In this study, we demonstrated that a more rapid and much simpler PCR-based method could be applied for determining triplex formation with genomic DNA, which might be extended to many other TFO related studies. A real-time PCR was used to quantify the triplex formation using two sets of primers, one set of primer for amplification of a control region and another for target region overlapping triplex forming site. A similar strategy has been shown successful in quantification of triplex formation in living cells (*23*, *33*). However, in our strategy, a gel elution procedure was used to remove unbound TFO molecules from the target DNA. In addition, a separate step for enriching triplex structure, e.g., using streptavidin-coated magnetic beads (*21*, *22*), is not required, since PCR can be efficiently inhibited by TFO-directed psoralen modification regardless of monoadduct or cross-linking (*21*, *26*, *34*, *46*). When we applied conventional PCR reaction to the samples without this purification step, we could detect the inhibition of PCR at a much lower TFO dose compared to those with purification step. This is because the unbound TFOs could bind to target sequence during PCR reaction and thus inhibit PCR reaction, resulting in overestimation of triplex formation, unless they are explicitly removed as suggested by Becker et al. (*47*). Even though Oh et al. were concerned that the unbound TFO might interfere with the accurate quantification of triplex formation (*21*), unbound TFOs might still persist in the reaction mixture using single-strand ligation PCR. Introduction of a purification step before real-time PCR, for both plasmid and naked genomic DNA, enabled us to detect triplex structures in around 80% of target sequence and 50% *in vivo*. This finding is consistent with other reports regarding the triplex formation efficiency *in vitro* (*22*, *32*, *33*) and *in vivo* (*20*, *23*) and confirmed the reliability of our method.

In conclusion, we demonstrated that triplex formation of APS165 with α1(I) collagen gene is possible, with high specificity and efficiency inside HSC-T6 cells. A very good correlation between the triplex formation and the gene inhibition was demonstrated with the help of a simple and quick real-time PCR-based method. The results from this study provide a consolidated base for the development of TFOs specific to α1(I) collagen gene promoter as antifibrotic agents. Furthermore, the described PCR-based assay can be generalized to other applications for detection of triplex formation.

REFERENCES

1. Casey, B. P., and Glazer, P. M. (2001) Gene targeting via triple-helix formation, *Prog. Nucleic Acid Res. Mol. Biol. 67*, 163−192.
2. Guntaka, R. V., Varma, B. R., and Weber, K. T. (2003) Triplex-forming oligonucleotides as modulators of gene expression, *Int. J. Biochem. Cell Biol. 35*, 22−31.
3. Noonberg, S. B., Francois, J. C., Garestier, T., and Helene, C. (1995) Effect of competing self-structure on triplex formation with purine-rich oligodeoxynucleotides containing GA repeats, *Nucleic Acids Res. 23*, 1956−1963.
4. Faria, M., and Giovannangeli, C. (2001) Triplex-forming molecules: from concepts to applications, *J. Gene Med. 3*, 299−310.
5. Rogers, F. A., Lloyd, J. A., and Glazer, P. M. (2005) Triplex-forming oligonucleotides as potential tools for modulation of gene expression, *Curr. Med. Chem.: Anti-Cancer Agents 5*, 319−326.
6. Kalish, J. M., and Glazer, P. M. (2005) Targeted genome modification via triple helix formation, *Ann. N.Y. Acad. Sci. 1058*, 151−161.
7. Cheng, K., Ye, Z., Guntaka, R. V., and Mahato, R. I. (2005) Biodistribution and hepatic uptake of triplex-forming oligonucleotides against type alpha1(I) collagen gene promoter in normal and fibrotic rats, *Mol. Pharmaceutics 2*, 206−217.
8. Grigoriev, M., Praseuth, D., Guieysse, A. L., Robin, P., Thuong, N. T., Helene, C., and Harel-Bellan, A. (1993) Inhibition of gene expression by triple helix-directed DNA cross-linking at specific sites, *Proc. Natl. Acad. Sci. U.S.A. 90*, 3501−3505.
9. Joseph, J., Kandala, J. C., Veerapanane, D., Weber, K. T., and Guntaka, R. V. (1997) Antiparallel polypurine phosphorothioate oligonucleotides form stable triplexes with the rat alpha1(I) collagen gene promoter and inhibit transcription in cultured rat fibroblasts, *Nucleic Acids Res. 25*, 2182−2188.
10. Intody, Z., Perkins, B. D., Wilson, J. H., and Wensel, T. G. (2000) Blocking transcription of the human rhodopsin gene by triplex-mediated DNA photocrosslinking, *Nucleic Acids Res. 28*, 4283−4290.
11. Faruqi, A. F., Datta, H. J., Carroll, D., Seidman, M. M., and Glazer, P. M. (2000) Triple-helix formation induces recombination in mammalian cells via a nucleotide excision repair-dependent pathway, *Mol. Cell. Biol. 20*, 990−1000.
12. Faria, M., Wood, C. D., Perrouault, L., Nelson, J. S., Winter, A., White, M. R., Helene, C., and Giovannangeli, C. (2000) Targeted inhibition of transcription elongation in cells mediated by triplex-forming oligonucleotides, *Proc. Natl. Acad. Sci. U.S.A. 97*, 3862−3867.
13. Besch, R., Giovannangeli, C., Kammerbauer, C., and Degitz, K. (2002) Specific inhibition of ICAM-1 expression mediated by gene targeting with Triplex-forming oligonucleotides, *J. Biol. Chem. 277*, 32473−32479.
14. Orson, F. M., Thomas, D. W., McShan, W. M., Kessler, D. J., and Hogan, M. E. (1991) Oligonucleotide inhibition of IL2R alpha mRNA transcription by promoter region collinear triplex formation in lymphocytes, *Nucleic Acids Res. 19*, 3435−3441.
15. Carbone, G. M., McGuffie, E., Napoli, S., Flanagan, C. E., Dembech, C., Negri, U., Arcamone, F., Capobianco, M. L., and Catapano, C. V. (2004) DNA binding and antigene activity of a daunomycin-conjugated triplex-forming oligonucleotide targeting the P2 promoter of the human c-myc gene, *Nucleic Acids Res. 32*, 2396−2410.
16. Asensio, J. L., Lane, A. N., Dhesi, J., Bergqvist, S., and Brown, T. (1998) The contribution of cytosine protonation to the stability of parallel DNA triple helices, *J. Mol. Biol. 275*, 811−822.
17. Macris, M. A., and Glazer, P. M. (2003) Transcription dependence of chromosomal gene targeting by triplex-forming oligonucleotides, *J. Biol. Chem. 278*, 3357−3362.
18. Espinas, M. L., Jimenez-Garcia, E., Martinez-Balbas, A., and Azorin, F. (1996) Formation of triple-stranded DNA at d(GA.TC)n sequences prevents nucleosome assembly and is hindered by nucleosomes, *J. Biol. Chem. 271*, 31807−31812.
19. Shahid, K. A., Majumdar, A., Alam, R., Liu, S. T., Kuan, J. Y., Sui, X., Cuenoud, B., Glazer, P. M., Miller, P. S., and Seidman, M. M. (2006) Targeted cross-linking of the human beta-globin gene in living cells mediated by a triple helix forming oligonucleotide, *Biochemistry 45*, 1970−1978.
20. Giovannangeli, C., Diviacco, S., Labrousse, V., Gryaznov, S., Charneau, P., and Helene, C. (1997) Accessibility of nuclear DNA to triplex-forming oligonucleotides: the integrated HIV-1 provirus as a target, *Proc. Natl. Acad. Sci. U.S.A. 94*, 79−84.
21. Oh, D. H., and Hanawalt, P. C. (1999) Triple helix-forming oligonucleotides target psoralen adducts to specific chromosomal sequences in human cells, *Nucleic Acids Res. 27*, 4734−4742.
22. Besch, R., Giovannangeli, C., Schuh, T., Kammerbauer, C., and Degitz, K. (2004) Characterization and quantification of triple helix formation in chromosomal DNA, *J. Mol. Biol. 341*, 979−989.
23. Brunet, E., Corgnali, M., Cannata, F., Perrouault, L., and Giovannangeli, C. (2006) Targeting chromosomal sites with locked nucleic acid-modified triplex-forming oligonucleotides: study of efficiency dependence on DNA nuclear environment, *Nucleic Acids Res. 34*, 4546−4553.
24. Majumdar, A., Puri, N., McCollum, N., Richards, S., Cuenoud, B., Miller, P., and Seidman, M. M. (2003) Gene targeting by triple helix-forming oligonucleotides, *Ann. N.Y. Acad. Sci. 1002*, 141−153.
25. Barre, F. X., Ait-Si-Ali, S., Giovannangeli, C., Luis, R., Robin, P., Pritchard, L. L., Helene, C., and Harel-Bellan, A. (2000) Unambiguous demonstration of triple-helix-directed gene modification, *Proc. Natl. Acad. Sci. U.S.A. 97*, 3084−3088.
26. Guieysse, A. L., Praseuth, D., Grigoriev, M., Harel-Bellan, A., and Helene, C. (1996) Detection of covalent triplex within human cells, *Nucleic Acids Res. 24*, 4210−4216.
27. Hanvey, J. C., Shimizu, M., and Wells, R. D. (1990) Site-specific inhibition of EcoRI restriction/modification enzymes by a DNA triple helix, *Nucleic Acids Res. 18*, 157−161.
28. Giovannangeli, C., Thuong, N. T., and Helene, C. (1992) Oligodeoxynucleotide-directed photo-induced cross-linking of HIV proviral DNA via triple-helix formation, *Nucleic Acids Res. 20*, 4275−4281.
29. Svinarchuk, F., Debin, A., Bertrand, J. R., and Malvy, C. (1996) Investigation of the intracellular stability and formation of a triple helix formed with a short purine oligonucleotide targeted to the murine c-pim-1 proto-oncogene promoter, *Nucleic Acids Res. 24*, 295−302.
30. Li, H., Broughton-Head, V. J., Peng, G., Powers, V. E., Ovens, M. J., Fox, K. R., and Brown, T. (2006) Triplex staples: DNA double-strand cross-linking at internal and terminal sites using psoralen-containing triplex-forming oligonucleotides, *Bioconjug Chem 17*, 1561−1567.
31. Bates, P. J., Macaulay, V. M., McLean, M. J., Jenkins, T. C., Reszka, A. P., Laughton, C. A., and Neidle, S. (1995) Characteristics of triplex-directed photoadduct formation by psoralen-linked oligodeoxynucleotides, *Nucleic Acids Res. 23*, 4283−4289.
32. Takasugi, M., Guendouz, A., Chassignol, M., Decout, J. L., Lhomme, J., Thuong, N. T., and Helene, C. (1991) Sequence-specific photo-induced cross-linking of the two strands of double-helical DNA by a psoralen covalently linked to a triple helix-forming oligonucleotide, *Proc. Natl. Acad. Sci. U.S.A. 88*, 5602−5606.
33. Musso, M., Wang, J. C., and Van Dyke, M. W. (1996) In vivo persistence of DNA triple helices containing psoralen-conjugated oligodeoxyribonucleotides, *Nucleic Acids Res. 24*, 4924−4932.
34. Giovannangeli, C., Thuong, N. T., and Helene, C. (1993) Oligonucleotide clamps arrest DNA synthesis on a single-stranded DNA target, *Proc. Natl. Acad. Sci. U.S.A. 90*, 10013−10017.
35. Raghow, R. (1994) The role of extracellular matrix in postinflammatory wound healing and fibrosis, *FASEB J. 8*, 823−831.
36. Nakanishi, M., Weber, K. T., and Guntaka, R. V. (1998) Triple helix formation with the promoter of human alpha1(I) procollagen gene by an antiparallel triplex-forming oligodeoxyribonucleotide, *Nucleic Acids Res. 26*, 5218−5222.
37. Ye, Z., Cheng, K., Guntaka, R. V., and Mahato, R. I. (2006) Receptor-mediated hepatic uptake of M6P-BSA-conjugated triplex-forming oligonucleotides in rats, *Bioconjugate Chem. 17*, 823−830.
38. Vogel, S., Piantedosi, R., Frank, J., Lalazar, A., Rockey, D. C., Friedman, S. L., and Blaner, W. S. (2000) An immortalized rat liver stellate cell line (HSC-T6): a new cell model for the study of retinoid metabolism in vitro, *J. Lipid Res. 41*, 882−893.
39. Kovacs, A., Kandala, J. C., Weber, K. T., and Guntaka, R. V. (1996) Triple helix-forming oligonucleotide corresponding to the polypyrimidine sequence in the rat alpha 1(I) collagen promoter specifically inhibits factor binding and transcription, *J. Biol. Chem. 271*, 1805−1812.
40. Guntaka, R. V., Richards, O. C., Shank, P. R., Kung, H. J., and Davidson, N. (1976) Covalently closed circular DNA of avian sarcoma virus: purification from nuclei of infected quail tumor cells and measurement by electron microscopy and gel electrophoresis, *J. Mol. Biol. 106*, 337−357.

41. Brenner, D. A., Rippe, R. A., and Veloz, L. (1989) Analysis of the collagen alpha 1(I) promoter, *Nucleic Acids Res. 17*, 6055−6064.
42. Dhalla, A. K., Kandala, J. C., Weber, K. T., and Guntaka, R. V. (1997) Identification of negative and positive regulatory elements in the rat alpha 1(I) collagen gene promoter, *Int. J. Biochem. Cell Biol. 29*, 143−151.
43. Rogers, F. A., Manoharan, M., Rabinovitch, P., Ward, D. C., and Glazer, P. M. (2004) Peptide conjugates for chromosomal gene targeting by triplex-forming oligonucleotides, *Nucleic Acids Res. 32*, 6595−6604.
44. Brunet, E., Corgnali, M., Perrouault, L., Roig, V., Asseline, U., Sorensen, M. D., Babu, B. R., Wengel, J., and Giovannangeli, C. (2005) Intercalator conjugates of pyrimidine locked nucleic acid-modified triplex-forming oligonucleotides: improving DNA binding properties and reaching cellular activities, *Nucleic Acids Res. 33*, 4223−4234.
45. Ram I Mahato, Z. Y., Ramareddy V Guntaka. (2004) Antisense and Antigene Oligonucleotides: Structure, Stability and Delivery, in *Biomaterials for Delivery and Targeting of Protein and Nucleic Acid Drugs* (Mahato, R. I., Ed.) pp 569−600, CRC Press, Boca Raton.
46. Hoepfner, R. W., and Sinden, R. R. (1993) Amplified primer extension assay for psoralen photoproducts provides a sensitive assay for a (CG)6TA(CG)2(TG)8 Z-DNA torsionally tuned probe: preferential psoralen photobinding to one strand of a B-Z junction, *Biochemistry 32*, 7542−7548.
47. Keiding, S., Badsberg, J. H., Becker, U., Bentsen, K. D., Bonnevie, O., Caballeria, J., Eriksen, J., Hardt, F., Keiding, N., Morgan, M., and et al. (1994) The prognosis of patients with alcoholic liver disease. An international randomized, placebo-controlled trial on the effect of malotilate on survival, *J. Hepatol. 20*, 454−460.

BI700580Y